Crystal structure and DFT calculations of 5-(4-Chlorophenyl)-1-(6-methoxy-pyridazin-3-yl)-1H-pyrazole-3-carboxylic acid

Can Alaşalvar, Mustafa Serkan Soylu, Hüseyin Ünver, Nazan Ocak İskeleli, Mustafa Yildiz, Murat Çiftçi, Erden Banoğlu

PII: S1386-1425(14)00777-X
DOI: http://dx.doi.org/10.1016/j.saa.2014.05.014
Reference: SAA 12168

To appear in: *Spectrochimica Acta Part A: Molecular and Biomolecular Spectroscopy*

Received Date: 27 March 2014
Revised Date: 30 April 2014
Accepted Date: 9 May 2014

Please cite this article as: C. Alaşalvar, M.S. Soylu, H. Ünver, N.O. İskeleli, M. Yildiz, M. Çiftçi, E. Banoğlu, Crystal structure and DFT calculations of 5-(4-Chlorophenyl)-1-(6-methoxypyridazin-3-yl)-1H-pyrazole-3-carboxylic acid, *Spectrochimica Acta Part A: Molecular and Biomolecular Spectroscopy* (2014), doi: http://dx.doi.org/10.1016/j.saa.2014.05.014

Crystal structure and DFT calculations of 5-(4-Chlorophenyl)-1-(6-methoxypyridazin-3-yl)-1H-pyrazole-3-carboxylic acid

Can Alaşalvar[a,*], Mustafa Serkan Soylu[b], Hüseyin Ünver[c], Nazan Ocak İskeleli[d], Mustafa Yildiz[e], Murat Çiftçi[f], Erden Banoğlu[f]

[a]*Giresun University, Technical Science Vocational High School, Department of Electric and energy, TR-28100,Giresun Turkey*
[b]*Department of Physics, Giresun University, TR-28100 Giresun, Turkey*
[c]*Department of Physics, Faculty of Science, Ankara University, TR-06100 Tandoğan, Ankara, Turkey*
[d]*Department of Science Education, Ondokuz Mayıs University, TR-55200 Atakum, Samsun, Turkey*
[e]*Department of Chemistry, Faculty of Science and Arts, Çanakkale Onsekiz Mart University, TR-17100 Çanakkale, Turkey*
[f]*Gazi University, Faculty of Pharmacy, Department of Pharmaceutical Chemistry, TR-06100 Besevler, Ankara, Turkey*

ABSRACT

The title compound, 5-(4-Chlorophenyl)-1-(6-methoxypyridazin-3-yl)-1H-pyrazole-3-carboxylic acid, has been characterized by using elemental analysis, MS, FT-IR, ^{1}H-NMR and ^{13}C-NMR spectroscopic, and crystallographic techniques. The title compound crystallizes in the triclinic space group P-1 with a = 9.612(1), b = 9.894(1), c = 17.380(1) Å, α= 90.213(5)°, β = 104.99(1)°, γ = 111.072(5)°, V = 1481.3(2) Å^3 and D_x = 1.483 g.cm^{-3} respectively. The structure of the compound has also been examined by using quantum chemical methods. The molecular geometry and vibrational frequencies of monomeric and dimeric form of the title compound in the ground state have been calculated by using the B3LYP/6-31G(d,p) level of the theory. The calculated results show that the optimized geometry and the theoretical vibration frequencies of the dimeric form are good agreement with experimental data. In addition, HOMO – LUMO energy gap, molecular electrostatic potential map, thermodynamic properties of the title compound were performed at B3LYP/6-31G (d,p) level of theory.

Key Words: Pyridazine and pyrazole core; Crystal structure; DFT, HOMO, LUMO

***Corresponding author. Tel: +900454 310 14 00**

E-mail adress: canalasalvar@hotmail.com (C. Alaşalvar)

Introduction

The pyridazine and pyrazole pharmacophores were often used as versatile scaffolds leading to a great variety of pharmacologically active compounds and certain derivatives bearing these scaffolds demonstrated good anti-platelet properties [1-6]. Moreover, small drug-like molecule libraries possessing vicinal diaryl template attracted great interest for many medicinal chemists for developing novel drug candidates and our research on vicinal diaryl systems produced a large number of compounds endowed with interesting pharmacological properties against cyclooxygenase and lipoxygenase pathways [7-11].

Besides of the developing of novel drug synthesis, the development of computational chemistry has contributed to the research of theoretical modeling of drug design, functional material design, etc., in a positive way over the past decade. For instance, it has become possible to guess the important physico-chemical properties of biological and chemical systems by varied computational techniques [12]. Recently, density functional theory (DFT) has been a milestone of theoretical modeling. Calculating many molecular properties with comparable accuracies to traditional correlated *ab-initio* methods with more plausible computational costs has become possible with the development of better and better exchange-correlation functional. The studies in the literature showed that the DFT has a perfect accuracy in reproducing the experimental values of in geometry, dipole moment, vibrational frequency, etc. [13, 14].

Pyridazine and pyrazole heterocyclic cores have good anti-platelet properties. Levent et all. synthesized and studied their against arachidonic acid (AA)-induced platelet aggregation and identified 5-(4-Chlorophenyl)-1-(6-methoxypyridazin-3-yl)-1H-pyrazole-3-carboxylic acid (Scheme 1) as a starting compound for further derivatization for the discovery of novel anti-platelet compounds [15]. But the crystal structure and theoretical calculations of this compound has not been studied yet. In this paper, the title compound was re-synthesized according to Ref. 15 and characterized by using FT-IR, single crystal X –ray and DFT methods. Hydrogen bond geometry of the molecule was determined by using X-ray difractometer. In addition, the properties of structural geometry, molecular electrostatic potential map, frontier orbitals and thermodynamic properties for the title compound were investigated at DFT/B3LYP/6-31G (d,p) level.

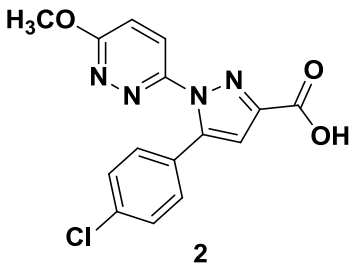

2

Scheme 1. Scaffold structure of the title compound

Experimental details

*Synthesis of Methyl 5-(4-chlorophenyl)-1-(6-chloropyridazine-3-yl)-1H-pyrazole-3-carboxylate **(1)***

To a mixture of methyl 4-(4-chlorophenyl)-2,4-dioxobutanoate (1 eq) and 6-chloro-3-hydrazino-pyridazine (1 eq) in 25 ml methanol, conc. HCl (0.5 eq) was added. After stirring at rt for 5 h, the precipitate was filtrated and recrystallized from methanol to yield **1** (75%). Mp 162-163^{o}C; IR (**ATR**): 3129, 3084, 2977, 1726, 1094 cm^{-1}; ^{1}H-NMR (DMSO-d_6): δ 3.87 (3H, s), 7.25 (1H, s), 7.37 (2H, d, J=8.4 Hz), 7.43 (2H, d, J=8.4), 8.18 (1H, d, J=8.8 Hz), 8.23 (1H, d, J=9.6 Hz); ^{13}C-NMR (DMSO-d_6): δ 52.86, 112.11, 127.68, 128.67, 129.22, 131.19, 132.58, 134.50, 145.21, 145.88, 155.72, 156.56, 162.12; HRMS **(m/z):** $[M+H]^+$ **calcd** for $C_{15}H_{11}Cl_2N_4O_2$: 349.0259; found 349.0257 [15].

*Synthesis of 5-(4-Chlorophenyl)-1-(6-methoxypyridazin-3-yl)-1H-pyrazole-3-carboxylic acid **(2)***

Compound **1** (1 eq) was dissolved in 20 ml methanol containing sodium methoxide (3 eq) and refluxed for 2.5 hours. Water was added (30 ml) and the reaction mixture was heated at reflux for another hour, diluted with water, and acidified. The precipitate formed was washed with water and recrystallized from ethanol-water mixture to yield 2 (82%). Mp 225-226^{o}C; IR (**ATR**): 3381, 2976, 2600, 1694, 1089 cm^{-1}; ^{1}H-NMR (DMSO-d_6): δ 4.04 (3H, s), 7.16 (1H, s), 7.34 (2H, d, J=8.8 Hz), 7.45 (2H, d, J=8.8), 7.52 (1H, d, J=9.2 Hz), 8.35 (1H, d, J=9.6 Hz), 13.23 (1H, bs); ^{13}C-NMR (DMSO-d_6): δ 55.74, 111.31, 120.92, 128.44, 128.94, 129.25, 131.03, 134.19, 144.65, 146.30, 152.79, 163.33, 165.36; HRMS **(m/z):** $[M+H]^+$ **calcd**

for $C_{15}H_{12}ClN_4O_3$: 331.0598; found 331.0602; Elemental Anal. Calcd for $C_{15}H_{11}ClN_4O_3$: C, 54.47; H; 3.35; N, 16.94; found C, 54.04; H, 3.31; N, 16.85.

As shown in Scheme 2, the 1,5-diarylpyrazole derivative (**1**) was synthesized by condensation of methyl 4-(4-chlorophenyl)-2,4-dioxobutanoate with 3-chloro-6-hydrazinylpyridazine in methanol in the presence of 0.5 eq HCl. Nucleophilic substitution of 6-chloro of pyridazine (**1**) with sodium methoxide followed by successive ester hydrolysis yielded 6-methoxypyridazine analogue in acid form (**2**) [15].

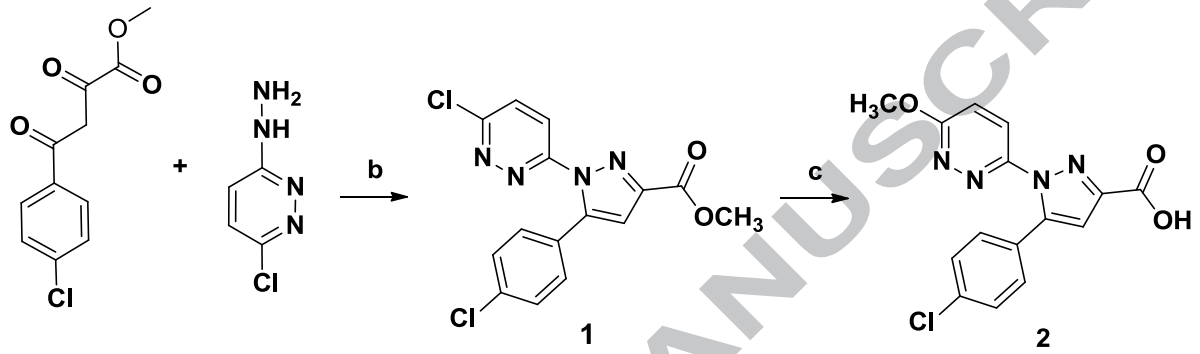

Scheme 2. Synthetic pathway for compound **2** [15].

Materials and measurements

All chemicals and reagents used in this study were purchased from Sigma-Aldrich Chemical Company (St Louis, MO, USA). IR spectrum was recorded on a Perkin-Elmer Spectrum one FT-IR spectrometer in KBr pellets.

Crystal data for the title compound (2)

X-ray diffraction data were recorded on a STOE IPDS II single crystal diffractometer (STOE & Cie GmbH, Darmstadt, Germany). The intensities collected were corrected for Lorentz and polarization factors, absorption correction by integration method via X-RED32 software [16]. The structure was solved by direct methods using SHELXS-97 [17] and refined with SHELXL-97 [17].

All non-hydrogen atoms were refined anisotropically. The refinement was carried out using the full matrix least squares method on the positional and anisotropic temperature parameters of non-hydrogen atoms corresponding to 425 crystallographic parameters. The

positions of the hydroxy H atoms were obtained from a difference map of the electron density in the unit-cell and were refined freely. All other hydrogen atoms were refined using a riding model with C–H = 0.93–0.96 Å. The constraint $U_{iso}(H) = 1.2U_{eq}$ (CH) or $1.5U_{eq}(CH_3)$ was applied. Details of the data collection conditions and the parameters of the refinement process are given in Table 1.

Computational details

We used Gauss – View molecular visualization program and Gaussian03 program package for the all calculations [18, 19]. Starting geometries of compound were taken from X-ray refinement data. The molecular structure of the compound in the ground state is optimized by using B3LYP/6-31G(d,p) level of the theory. In DFT calculation, hybrid functional are also used, the Becke's three parameter functional (B3) [20] which defines the exchange functional as the linear combination of Hartre- Fock, local and gradient – corrected exchange terms. The B3 hybrid functional was used in combination with the correlation functional of Lee, Yang and Parr [21]. For the compound, vibration frequencies were calculated by using DFT/B3LYP with 6-31G (d,p) basis set. The Calculated frequencies were scaled by 0.9627 [22]. Both geometries of the title compound and tetramethylsilane (TMS) were fully optimized. ^{1}H and ^{13}C chemical shifts were computed. The standard GIAO/B3LYP/6-31G(d) (Gauge-Independent Atomic Orbital) approach [23-24] applying B3LYP level 6-31G(d,p) basic set was used for these calculations. The ^{1}H and ^{13}C NMR chemical shifts are converted into the TMS scale by subtracting the calculated absolute chemical shielding of TMS ($\delta = \Sigma_0 - \Sigma$, where δ is the chemical shift, Σ is the absolute shielding and Σ_0 is the absolute shielding of TMS), whose values is 31.76 ppm and 191,81 ppm for B3LYP/6-31G(d,p) level of the theory, respectively. In addition, MEP map, HOMO – LUMO energy values and thermodynamic properties of the title compound were calculated by using B3LYP/6-31G(d,p) level of the theory.

Results and discussions

Crystallographic study

The title compound **(2)** crystallizes in the triclinic space group P-1, an Olex-2 [25] view of **(2)** is shown in Fig. 1 and Crystal data, data collection and refinement details for the

title compound were given in Table 1. The asymmetric unit in the crystal structure contains two independed similar molecules. The title compound consists of a pyrazole-3-carboxylic acid ring with 4-chlorophenyl and 6-methoxypyridazin substituents at the 1- and 5-positions, respectively.

All bond distances in the pyrazole ring indicate partial double bond character, which suggests a delocalized π-electronic system throughout the ring [26]. Glancing at the Table 2, the C3=C4 distance of 1.370(2) Å is slightly deviates from the average C=C double bond length (average for C=C sp^2=sp^2 bond is 1.34 Å). The C2-C3 bond length of 1.395(2) Å is slightly shorter than the pure C-C sp^2-sp^2 single bond (average length for such a bond is 1.48 Å) [27]. Moreover, the N=N bond length is shorter than those found in the above-cited structures [N=N 1.373(2) Å 1.380(8) Å] [28].

For two molecules in the asymmetric unit, the dihedral angles between pyridazine and phenyl rings, in an interesting way, is quite different. While the dihedral angle between (C5-C10) and (C11-C12-C13-C14-N3-N4) mean planes is 48, 75º (10), the angle between (C5A-C10A) and (C11A-C12A-C13A-C14A-N3A-N4A) mean planes is 84, 95º (12).

Hydrogen bond geometry values of the title compound are given Table 3. In the packing of the title compound, two independed asymmetric units are connected by the O1-H1…O2A and O1A-H1A…O2 hydrogen bonds into centro symmetric dimers resulting in $R_2^2(8)$ ring motifs, as depicted in Fig.2 [29].

Optimized geometry

The optimized parameters (bond lengths, bond angles, and dihedral angles) of monomer and dimer forms of the title compound were obtained at B3LYP level with the 6-31G (d,p) basis set and listed with experimental values in Table 2. The optimized molecular structures of monomer and dimer forms of the title compound are shown in Fig. 3 (a) and (b), respectively. Glancing at Table 2; C1 – O1, C1 – O2 bond lengths were calculated as 1.314, 1.236 Å and as 1.350, 1.215 Å for the dimeric form and monomeric form respectively. These bond distances (C1 – O1 and C1 – O2) were observed as 1.285, 1.230 Å. Calculated bond parameters for dimeric form are consistent with the experimental values, whereas the calculated values for monomeric form deviates from experimental values especially on the carboxylic acid group of the title molecule. The reason of these deviations, it can be intramolecular hydrogen bond interactions in given Table 3.

Intramolecular interactions values in the title compound are calculated by using B3LYP/6-31G (d,p) method and listed Table 4. Calculated and experimental hydrogen bond interactions values are compatible with each other.

FT-IR and NMR spectra analyses

Vibrational frequencies of the title compound of monomer and dimeric form are calculated by using DFT with 6-31G (d,p) basic set and some important vibration modes are listed in Table 5, with their experimental values. FT – IR spectrum is shown in Fig. 4. The carboxylic group (–COOH) of the title compound contains the C–O, C=O and O–H vibrational modes. The very board peak observed between 2500–3300 cm^{-1} in IR spectrum can be assigned to the O–H stretching vibration mode in the title molecule. But weak C–H stretching bands occur in this region (near 3000 cm^{-1}) and seen over of O–H band. O–H stretching band was observed as 2990cm^{-1} in the Fig. 4. This band was calculated as 3619cm^{-1} and 2995cm^{-1} for monomer and dimer form of the title compound, respectively. The C=O stretching band appears strongly in the region 1870–1540 cm^{-1} in which the position of C=O stretching band depends on the physical state, electronic and mass effects of neighboring substituents, conjugations and intramolecular and intermolecular hydrogen bonding [30–35]. C=O stretching band in the Fig. 4 was observed as 1697cm^{-1}. This band was calculated as 1753cm^{-1} and 1694cm^{-1} for monomeric and dimeric form of the title compound, respectively. Calculated values for O–H and C=O vibration of monomer form of title compound are bigger than experimental values. This situation can be explained by the presence of O… H – O strong intramolecular hydrogen bond given Table 3. As seen Table 5, calculated O–H and C=O vibration values of dimeric form are in good agreement with experimental values.

The O – CH_3 stretching vibration bands of methoxy group for the title compound is observed at 1009cm^{-1}, and this band for monomer and dimer form are found at 1004 and 1003cm^{-1} in our B3LYP/6-31G(d,p) calculations, respectively. The obtained results are in a good agreement with literature [36-38].

The C – H, C – H_3 and C – C vibration modes have been calculated at 3080 – 3172cm^{-1} (C –H stretching), 2947 – 3052cm^{-1} (C – H_3 stretching) and 1593cm^{-1} (C – C stretching) for the dimeric form and 3081 – 3171cm^{-1}, 2947 – 3053cm^{-1} and 1588cm^{-1} for monomeric form and these bands are observed at 2955-3086, 2594-2880 and 1598cm^{-1} respectively.

The C – N + C – C stretching in the pyridazine ring for the monomeric and dimeric form are computed at 1543cm^{-1} and 1546cm^{-1} respectively and this mode is observed at

1544cm^{-1}. In the pyrazole ring, the C - N + C - C and C – N - C + C – N - N stretching modes are calculated as 1430, 1399 cm^{-1} for monomeric form and 1432, 1411 cm^{-1} for dimeric form, while these modes are observed as 1469 and 1409 cm^{-1} respectively.

Structural analysis of the compound was carried out with the help of ^{1}H-NMR and ^{13}C-NMR using DMSO-d_6. Observed and calculated ^{1}H-NMR and ^{13}C-NMR chemical shift values are given at Table 6. According to Table 6, theoretical and experimental values of ^{1}H and ^{13}C NMR of the molecule are in good agreement except H atom the bounded to Oxygen atom. Because of this, it can be O – H…O intramolecular interactions given in Table 3.

Molecular electrostatic potential analysis

The molecular electrostatic potential (MEP), *V(r)* at a given point *r(x, y, z)* in the vicinity of a molecule, is defined in terms of the interaction energy between an electrical charge which is generated from the molecule electrons and nuclei and a positive test charge(a proton) located at *r*. For the system studied, the *V(r)* values are calculated by the equation [39],

$$V(r) = \sum_{A} \frac{Z_A}{(R_A - r)} - \int \frac{\rho(r')}{|r' - r|} dr'$$

where Z_A is the charge of nucleus *A* located at R_A, $\rho(r')$ is the electronic density function of the molecule, and r' is the dummy integration variable. To predict the reactive sites of electrophilic and nucleophilic attack for the investigated molecule, the MEP at the B3LYP/6-31G(d,p) optimized geometry of monomeric form was calculated and shown in Fig. 5. As seen from Fig.5, the most negative regions are located on the O1 atom which can be considered as possible site for electrophilic attack and its *V(r)* value is -0.042a.u. Other negative region is located on the N1 atom and *V(r)* values are -0.040 a.u.. However, the maximum positive region is located on the H atom bonded O2 atom and *V(r)* value is 0.052a.u. This indicates a possible site for nucleophilic attack. The MEP is related to the electronic density and is a very useful descriptor for determining sites for electrophilic attack and nucleophilic reactions as well as hydrogen-bonding interactions [40-43]. So, Fig.5 supports the existence of the intramolecular interactions given in Table 3.

HOMO - LUMO analysis

The most important orbitals in a molecule are the frontier molecular orbitals, called HOMO and LUMO. HOMO implies that the outermost orbital filled by electrons, and behaves as an electron donor while LUMO can be thought as the first empty innermost orbital unfilled by electron and behaves as an electron acceptor. The energy of the HOMO is directly related to the ionization potential and represents the ability of electron giving. But, LUMO energy is directly related to the electron affinity and represents the ability of electron accepting. The formed energy gap between HOMO and LUMO indicates the molecular chemical stability [44]. The energy gap between HOMO and LUMO is a critical parameter to determine molecular electrical transport properties. By using HOMO and LUMO energy values for a molecule, chemical hardness–softness, electronegativity and electrophilicity index can be calculated as follows:

$$\mu \approx -\chi = -\frac{I+A}{2} \quad \text{(Electronegativity)}$$

$$\eta \approx \frac{I-A}{2} \quad \text{(Chemical hardness)}$$

$$\zeta = \frac{1}{2\eta} \quad \text{(Softness)}$$

$$\psi = \frac{\mu^2}{2\eta} \quad \text{(Electrophilicity index)}$$

Where I and A is ionization potential and electron affinity, and is $I = -E_{HOMO}$ and $A = -E_{LUMO}$, respectively [45-48]. Molecules which have a large HOMO–LUMO energy gap are called “hard” and which have a small HOMO–LUMO energy gap are called “soft”. Frontier orbitals (HOMO – LUMO) of the title molecule were calculated by using B3LYP/6-31G(d,p) method in gas phase. HOMO–LUMO energy gap, electronegativity, electrophilicity index and chemical hardness and softness values of monomer and dimer form of title molecule were listed in Table 7. The band gap energy of the one electron excitation from HOMO to LUMO for monomer and dimer form is calculated about 4.68 eV and 4.59eV respectively. This large HOMO–LUMO gap is an indication of a good stability and a high chemical hardness for the title compound. For monomer and dimer form, 3D plots of highest occupied molecular orbitals (HOMO), lowest unoccupied molecular orbitals (LUMO) were shown in Fig. 6.

Thermodynamic Properties

All the thermodynamic calculations have been carried out in gas phase and they could not be used in solution. Standard thermodynamic function: heat capacity ($C^o_{p,m}$), entropy (S^o_m) and enthalpy (H^o_m) based on vibrational analysis at the B3LYP/6-31G(d,p) level were obtained and listed Table 8. The Table 8 indicates that standard heat capacity, entropies and enthalpies increase at any temperatures from 200K to 500K, because the intensities of the molecular vibration increase with increasing temperature. The correlation equations between these thermodynamic parameters ($C^0_{p,m}$, S^0_m , H^0_m) and temperature T are as follows:

$C^o_{p,m} = -1x10^{-4}T^2 + 0.2785T - 1.9177$ (R^2=0.9981)

$S^o_m = -5x10^{-5}T^2 + 0.2863T + 70.607$ (R^2=0.9989)

$H^o_m = 1x10^{-4}T^2 + 0.0145T - 0.5016$ (R^2=0.9998)

Conclusions

5-(4-Chlorophenyl)-1-(6-methoxypyridazin-3-yl)-1H-pyrazole-3-carboxylic acid has been characterized by using FT-IR and X-ray technique experimentally and using B3LYP/6-31G(d,p) method theoretically. Molecular geometry parameters and vibrational frequencies values were calculated using B3LYP/6-31G(d,p) method for monomeric and dimeric form of the compounds. Calculated values in the dimeric form were found to be more compatible with experimental data. The MEP map shows that the negative potential sites are on electronegative atoms as well as the positive potential sites are around the hydrogen atoms. These sites give information about the region from where the compound can have intermolecular and intramolecular interactions. For monomer and dimer form, HOMO-LUMO energy gap of the molecule are 4.68eV and 4.59eV respectively. This large HOMO–LUMO gap is an indication of a good stability and a high chemical hardness for the title compound. In addition, the correlations between the thermodynamic parameters ($C^0_{p,m}$, S^0_m , H^0_m) and temperatures T were also obtained.

Supplementary material

Crystallographic data for the structures reported in this article have been deposited with the Cambridge Crystallographic Data Centre as supplementary publication number 970299 (title compound). Copies of the data can be obtained free of charge on application to CCDC 12 Union Road, Cambridge CB21 EZ, UK. Fax: +44 1223 336 033; e-mail: data_request@ccdc.cam.ac.uk.

References

[1]. A. Coelho, E. Sotelo, N. Fraiz, M. Yanez, R. Laguna, E. Cano, E. Ravina, Bioorg. Med. Chem. Lett. 14 (2004) 321-324.

[2]. T. Costas, P. Besada, A. Piras, L. Acevedo, M. Yanez, F. Orallo, R. Laguna, C. Teran, Bioorg. Med. Chem. Lett. 20 (2010) 6624-6627.

[3]. A. Crespo, C. Meyers, A. Coelho, M. Yanez, N. Fraiz, E. Sotelo, B.U. Maes, R. Laguna, E. Cano, G.L. Lemiere, E. Ravina, Bioorg. Med. Chem. Lett. 16 (2006) 1080-1083.

[4]. P.I. Dosa, S. Strah-Pleynet, H. Jayakumar, M. Casper, M. Decaire, Y. Xiong, J. Lehmann, K. Choi, K. Elwell, A. Wong, R.R. Webb, J.W. Adams, J. Ramirez, J.G. Richman, W. Thomsen, G. Semple, B.R. Teegarden, Bioorg. Med. Chem. Lett. 19 (2009) 5486-5489.

[5]. R. Ferroni, L. Milani, D. Simoni, P. Orlandini, M. Guarneri, D. Franze, A. Bardi, Farmaco. 44 (1989) 495-502.

[6]. K. Rehse, J. Kotthaus, L. Khadembashi, Arch. Pharm. (Weinheim). 342 (2009) 27-33.

[7]. B. Caliskan, S. Luderer, Y. Ozkan, O. Werz, E. Banoglu, Eur. J. Med. Chem. 46 (2011) 5021-5033.

[8]. Y. Dundar, S. Unlu, E. Banoglu, A. Entrena, G. Costantino, M.T. Nunez, L. Labeaga, M.F. Sahin, N. Noyanalpan, Eur. J. Med. Chem. 44 (2009) 1830-1837.

[9]. G. Eren, S. Unlu, M.T. Nunez, L. Labeaga, F. Ledo, A. Entrena, E. Banoglu, G. Costantino, M.F. Sahin, Bioorg. Med. Chem. 18 (2010) 6367-6376.

[10]. B.C. Ergun, M.T. Nunez, L. Labeaga, F. Ledo, J. Darlington, G. Bain, B. Cakir, E. Banoglu, Arzneimittelforschung. 60 (2010) 497-505.

[11]. S. Unlu, E. Banoglu, S. Ito, T. Niiya, G. Eren, B. Okcelik, M.F. Sahin, J. Enzyme Inhib. Med. Chem. 22 (2007) 351-361.

[12] Y. Zhang, Z.J. Guo, X.Z. You, J. Am. Chem. Soc. 123 (2001) 9378−9387.

[13] G. Fitzgerald, J. Andzelm, J. Phys. Chem. 95 (1991) 10531−10534.

[14] H. Tanak, Int. J. Quant. Chem. 112 (2011) 2392−2402.

[15] S. Levent, B. Çalışkan, M. Çiftci, Y. Özkan, İ. Yenicesu, H. Ünver, E. Banoğlu, Eur. J. Med. Chem. 64(2013) 42-53

[16] Stoe & Cie X-AREA (Version 1.18) X-RED32 (Version 1.04), Stoe&Cie, Darmstadt, Germany, 2002.

[17] G.M. Sheldrick, SHELXS97, SHELXL97, University of Gottingen, Germany, 1997.

[18] M. J. Frisch, G. W. Trucks, H. B. Schlegel, G. E. Scuseria, M. A. Robb, J. R. Cheeseman, J. A. Montgomery, Jr., T. Vreven, K. N. Kudin, J. C. Burant, J. M. Millam, S. S. Iyengar, J. Tomasi, V. Barone, B. Mennucci, M. Cossi, G. Scalmani, N. Rega, G. A. Petersson, H. Nakatsuji, M. Hada, M. Ehara, K. Toyota, R. Fukuda, J. Hasegawa, M. Ishida, T. Nakajima, Y. Honda, O. Kitao, H. Nakai, M. Klene, X. Li, J. E. Knox, H. P. Hratchian, J. B. Cross, V. Bakken, C. Adamo, J. Jaramillo, R. Gomperts, R. E. Stratmann, O. Yazyev, A. J. Austin, R. Cammi, C. Pomelli, J. W. Ochterski, P. Y. Ayala, K. Morokuma, G. A. Voth, P. Salvador, J. J. Dannenberg, V. G. Zakrzewski, S. Dapprich, A. D. Daniels, M. C. Strain, O. Farkas, D. K. Malick, A. D. Rabuck, K. Raghavachari, J. B. Foresman, J. V. Ortiz, Q. Cui, A. G. Baboul, S. Clifford, J. Cioslowski, B. B. Stefanov, G. Liu, A. Liashenko, P. Piskorz, I. Komaromi, R. L. Martin, D. J. Fox, T. Keith, M. A. Al-Laham, C. Y. Peng, A. Nanayakkara, M. Challacombe, P. M. W. Gill, B. Johnson, W. Chen, M. W. Wong, C. Gonzalez, and J. A. Pople, Gaussian 03, Gaussian, Inc., Pittsburgh PA., 2003.

[19] A. Frisch, I.I.R. Dennington, T. Keith, J. Millam, A.B. Nielsen, A.J. Holder, J. Hiscocks, Reference, Version 4.0, Gaussian Inc., Pittsburgh, 2007.

[20] AD Becke, J. Chem. Phys. 98(1993) 5648–5652

[21] C Lee, W. Yang, RG Parr, Phys. Rev. B 37 (1988) 785–789

[22] A.P. Scott, L. Radom, J. Phys Chem. 100 (1996) 16502.

[23] Ditchfield R (1972) J Phys Chem 56 :5688

[24] Wolinski K, Hinton J F, Pulay P (1990) J Am Chem Soc 112 : 8251

[25] O V Dolomanov , L. J. Bourhis, R. J. Gildea, J. A. K. Howard, H. Puschmann, "*OLEX2*: a complete structure solution, refinement and analysis program". J. Appl. Cryst. (2009) 42, 339-341.

[26] T. Eicher, S. Hauptmann, The Chemistry of Heterocycles Structure, Reactions, Syntheses and Applications, Second, Completely Revised, and Enlarged Edition, WILEY-VCH GmbH & Co. KGaA, Weinheim, 2003

[27] M.B. Smith, J. March, March, March’ s Advanced Organic Chemistry Reactions,echanisms, and Structure, sixth ed., John Wiley & Sons, Inc., 2007

[28] C.J. Fahrni, L.C. Yang, Van Derveer, J. Am. Chem. Soc. 125 (2003) 3799

[29] Bernstein, J., Davis, R. E., Shimoni, L. & Chang, N.-L. (1995). Angew. Chem. Int. Ed. Engl. 34, 1555-1573

[30] B.H. Stuart, *Infrared Spectroscopy: Fundamentals and Applications* (JohnWilley & Sons, England, 2004).

[31] R.M. Silverstein and F.X. Webster, *Spectroscopic Identification of Organic Compound*, 6nd edn. (John Willey & Sons, New York, 1998).

[32] G. Varsanyi, *Vibrational Spectra of Benzene Derivatives* (Academic Press, New York, 1969).

[33] D.L. Pavia, G.M. Lampman, G.S. Kriz and J.R. Vyvyan, *Introduction to Spectroscopy* (BROOKS/COLE CENGAGE Learing, USA, 2009).

[34] L.J. Bellamy, *The Infrared Spectra of Complex Molecules*, 3rd edn. (Wiley, New York, 1975).

[35] N.B. Colthup, L.H. Daly and E. Wiberley, *Introduction to Infrared and Raman Spectroscopy* (Academic Press, New York, 1964).

[36] A. Abbas, S. Bahçeli, H. Gökçe, M. Bolte, S. Hussain, M.K. Rauf, Spectrochimica Acta Part A 116 (2013) 599–609.

[37] H. Gökçe, O. Akyıldırım, S. Bahçeli, H.Yüksek, Ö.G. Kol, Journal of Molecular Structure 1056 (2014) 273-284.

[38] H. Gökçe, S. Bahçeli, O. Akyıldırım, H. Yüksek, Ö.G. Kol, Lett. Org. Chem. 10 (2013) 395-441.

[39] P. Politzer, J.S. Murray, Theor. Chem. Acc. 108 (2002) 134–142.

[40] A. Tokatlı, E. Özen, F. Ucun, S. Bahçeli, Spectrochim. Acta A 78 (2011) 1201–1211.

[41] E. Scrocco, J. Tomasi, Adv. Quantum Chem. 11 (1979) 115–121.

[42] F.J. Luque, J.M. Lopez, M. Orozco, Theor. Chem. Acc. 103 (2000) 343–345.

[43] N. Okulik, A.H. Jubert, Internet Electron J. Mol. Des. 4 (2005) 17–30.

[44] K. Fukui, Science 218 (4574) (1982) 747−754.

[45] H. Gökçe, S. Bahçeli, Spectrochim. Acta A 114 (2013) 61-73

[46] W. Kohn, A.D. Becke, R.G. Parr, J. Phys. Chem. 100 (31) (1996) 12974−12980.

[47] R.G. Parr, R.G. Pearson, J. Am. Chem. Soc. 105 (26) (1983) 7512−7516.

[48] R.G. Pearson, Proc. Natl. Acad. Sci. USA 83 (22) (1986) 8440−8441.

Figure Captions

Fig. 1. Olex 2 plots of dimeric form of the title compound with atom numbering schemes. Displacement ellipsoids are represented at 50% probability levels. H atoms are shown as small spheres of arbitrary radius.

Fig. 2. Packing diagram of the title compound

Fig. 3. Theoretical structure of the title compound (a) Dimeric form (b)monomeric form

Fig. 4. FT-IR spectrum of the title compound

Fig. 5. Molecular Electrostatic Potential (MEP) Map of the title compound

Fig. 6. For title compound 3D plots of (a)HOMO; (b)LUMO

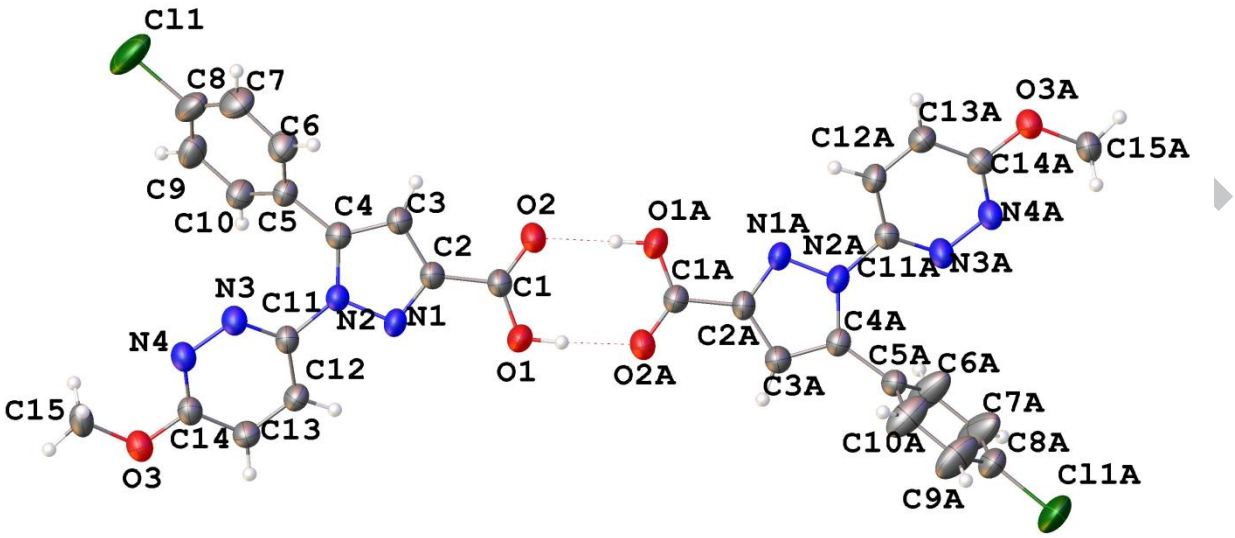

Fig. 1. Olex 2 plots of dimeric form of the title compound with atom numbering schemes. Displacement ellipsoids are represented at 50% probability levels. H atoms are shown as small spheres of arbitrary radius.

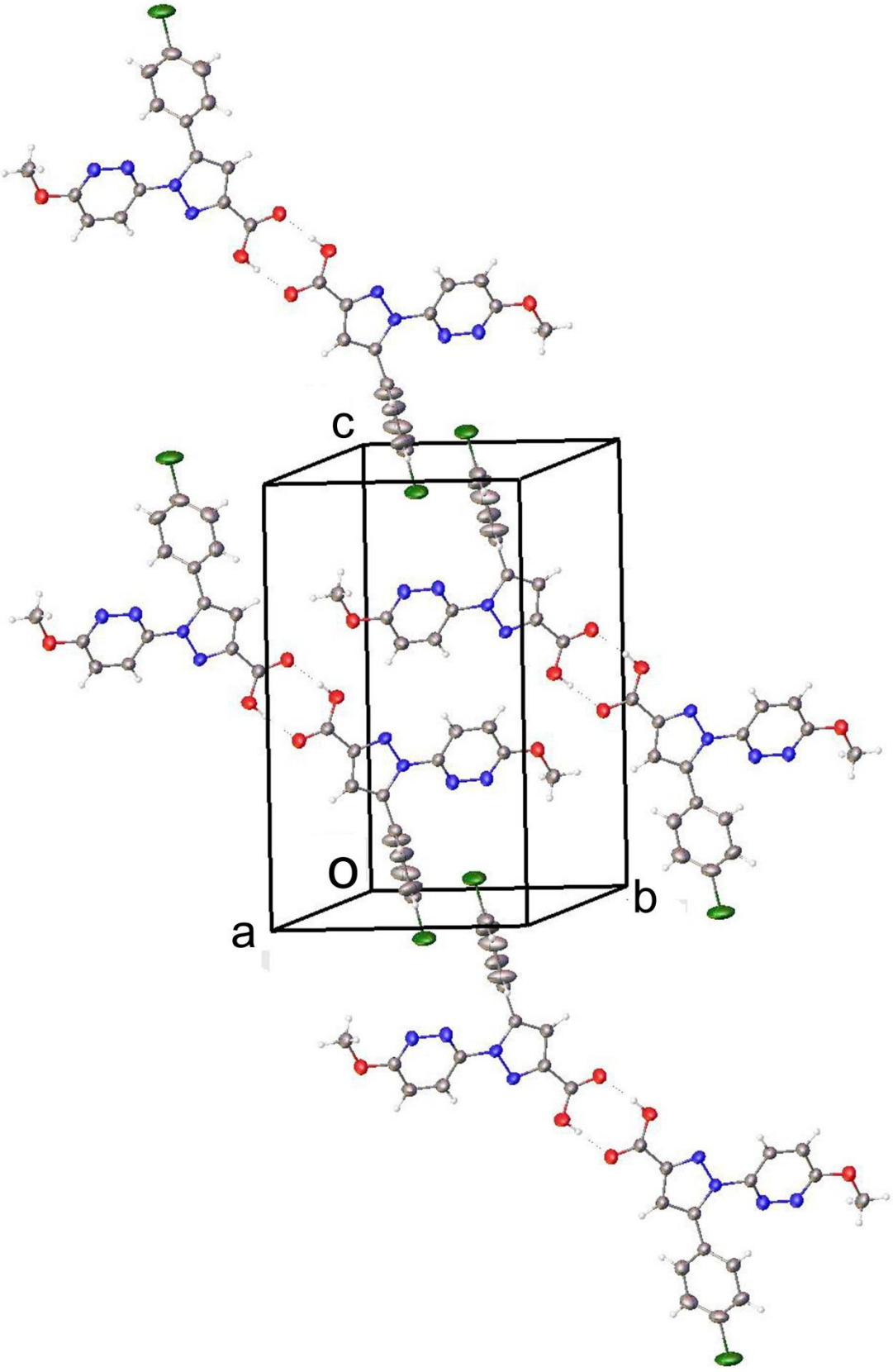

Fig. 2. Packing diagram of the title compound

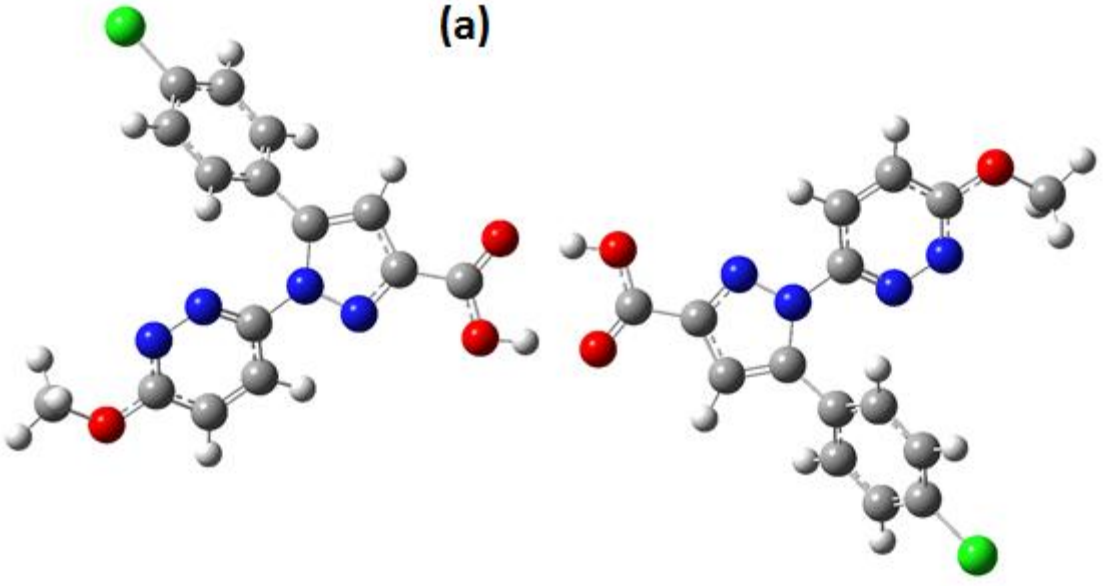

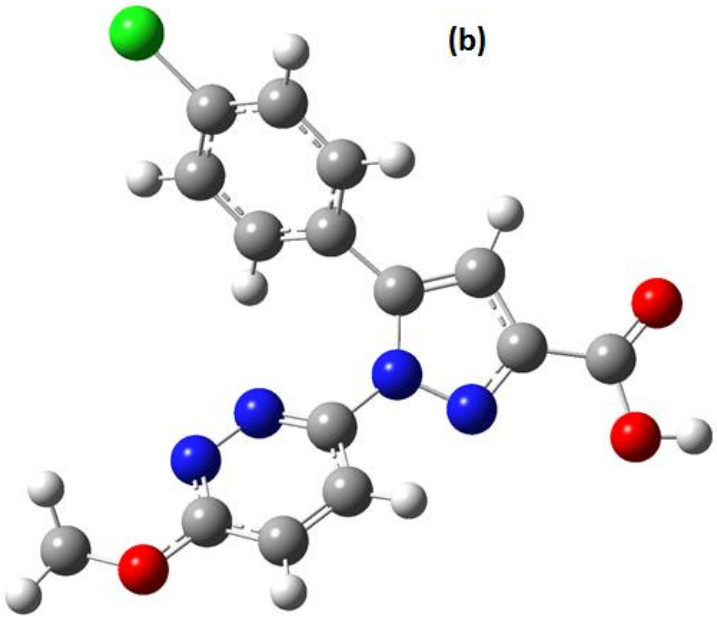

Fig. 3. Theoretical structure of the title compound (a) Dimeric form (b)monomeric form

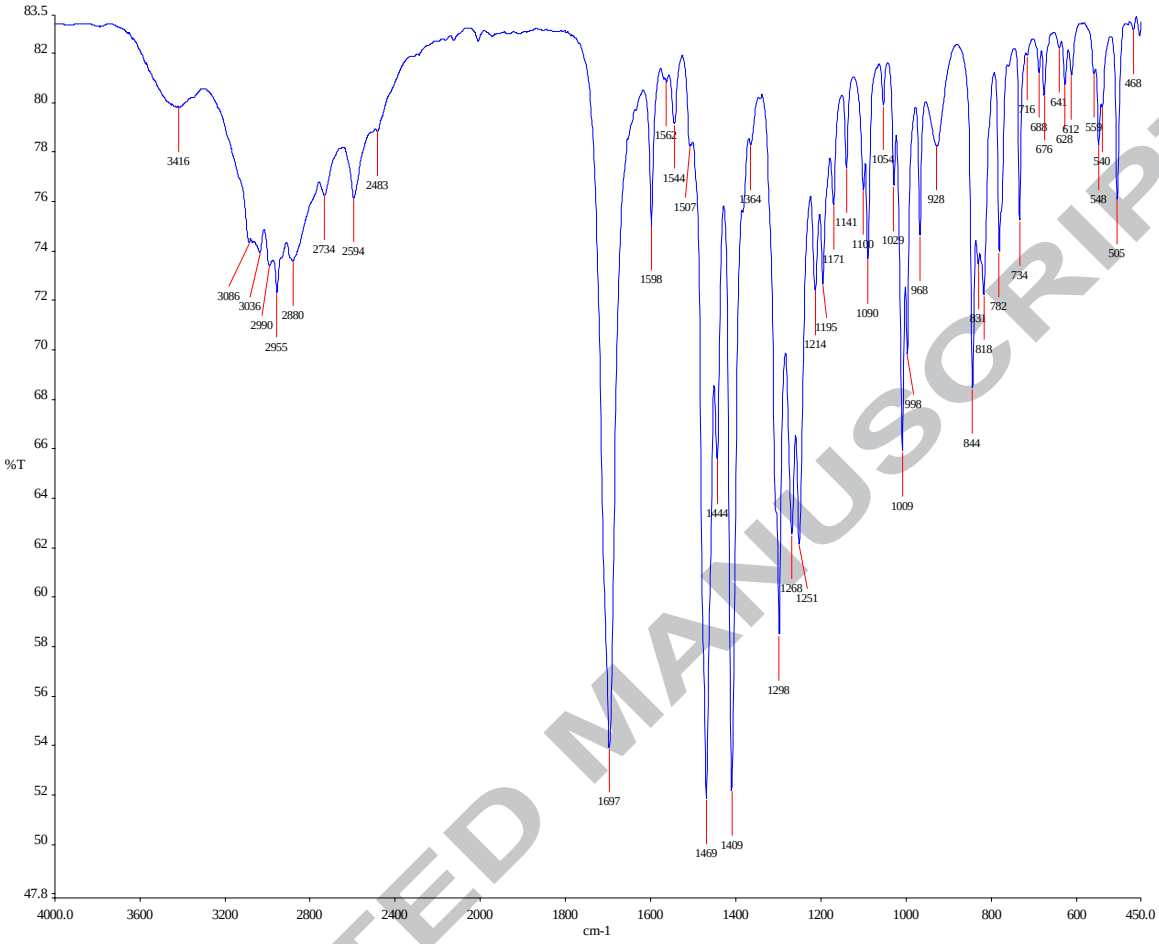

Fig. 4. FT-IR spectrum of the title compound

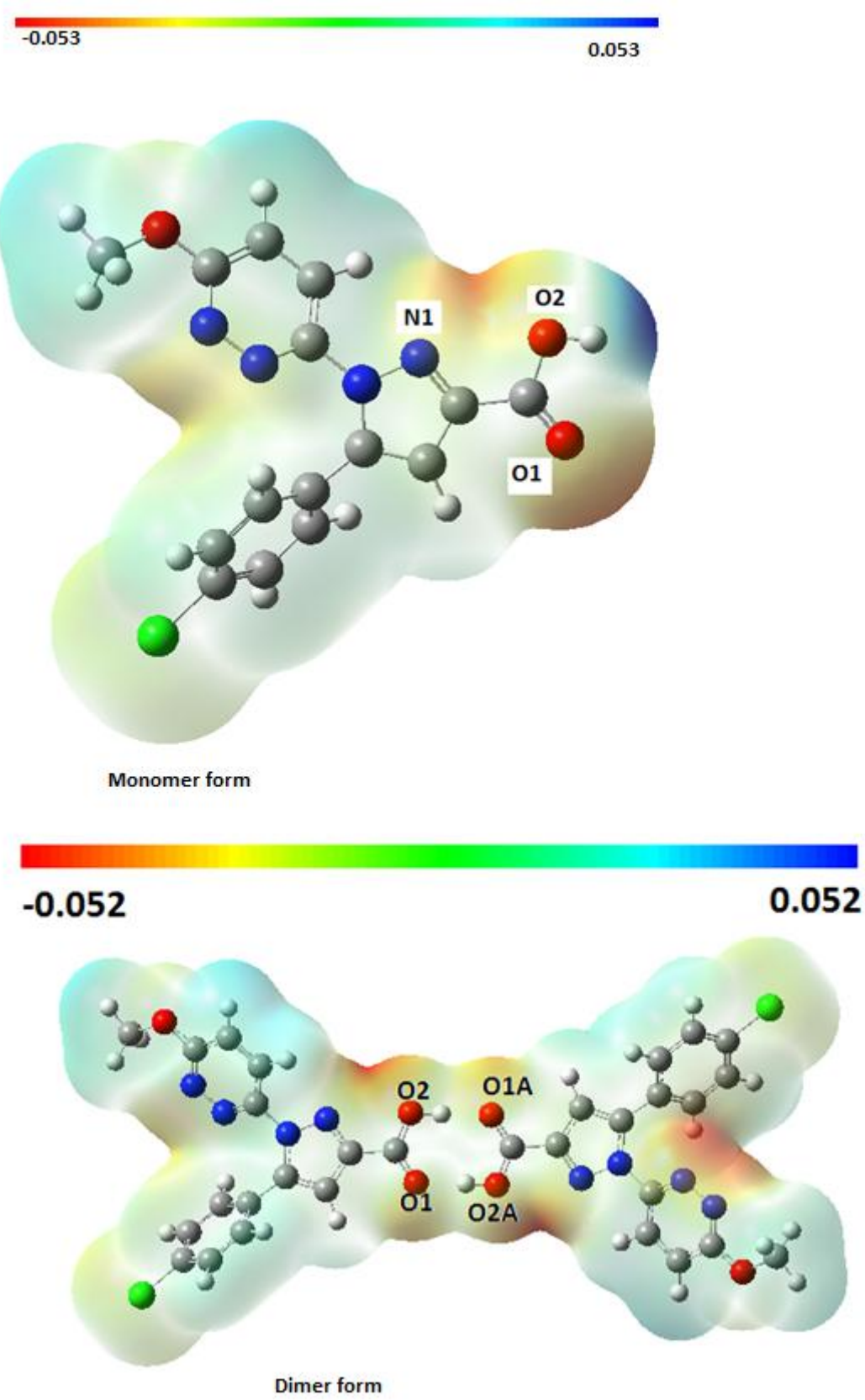

Fig. 5. Molecular Electrostatic Potential (MEP) Map of the title compound (dimeric and monomer form)

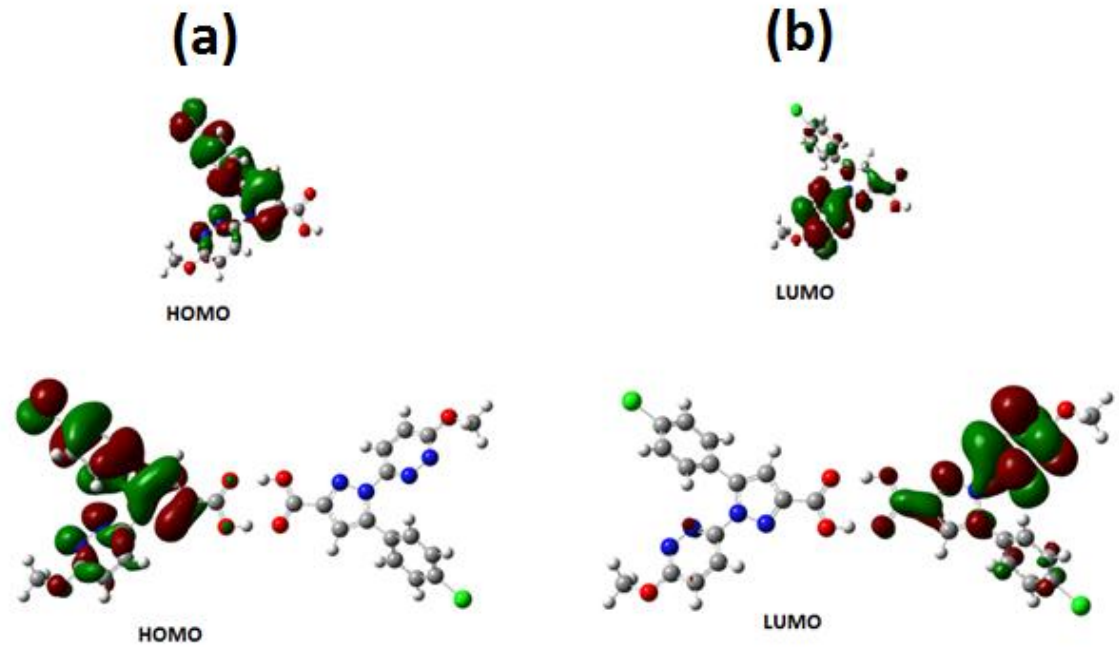

Fig. 6. For title compound 3D plots of (a) HOMO; (b) LUMO

Table 1

Crystal data, data collection and refinement detail for the title compound

Empirical formula	$C_{30}H_{22}Cl_2N_8O_6$
Formula weight	661.46
Temperature/K	293(2)
Crystal system	triclinic
Space group	P-1
a/Å	9.612(1)
b/Å	9.894(1)
c/Å	17.380(1)
α/°	90.213(5)
β/°	104.987(5)
γ/°	111.072(5)
Volume/$Å^3$	1481.3(2)
Z	2
ρ_{calc} mg/mm^3	1.483
μ/mm^{-1}	0.279
F(000)	680.0
Crystal size/mm^3	0.28 × 0.21 × 0.18
2θ range for data collection	4.44 to 53.66°
Index ranges	$-12 \le h \le 12$, $-12 \le k \le 12$, $-21 \le l \le 21$
Reflections collected	21520
Independent reflections	6297[R(int) = 0.0498]
Data/restraints/parameters	6297/0/425
Goodness-of-fit on F^2	0.879
Final R indexes [I>=2σ (I)]	R_1 = 0.0492, wR_2 = 0.1017
Final R indexes [all data]	R_1 = 0.1313, wR_2 = 0.1240
Largest diff. peak/hole / e $Å^{-3}$	0.28/-0.29

Table 2
Selected molecular structure parameters

Parameters	**Experimental**	**B3LYP/6-31G(d,p)**	
		Monomer	**Dimer**
Bond lengths (Å)			
C1—O2	1.230 (3)	1.215	1.236
C1—O1	1.285 (3)	1.350	1.314
C1A—O2A	1.230 (3)	-	1.236
C1A—O1A	1.287 (3)	-	1.314
C1—C2	1.469 (3)	1.476	1.476
N1—N2	1.361 (2)	1.352	1.351
N1—C2	1.323 (3)	1.332	1.332
N2—C4	1.374 (3)		1.391
N3—N4	1.358 (3)	1.339	1.339
Cl1—C8	1.746 (3)	1.758	1.758
Cl1A—C8A	1.744 (3)	-	1.757
Bond angles (°)			
C2—C1—O1	116.3 (2)	113.56	115.14
C2—C1—O2	119.5 (2)	123.29	119.99
N2—C4—C5	127.2 (2)	128.08	128.21
C4—N2—C11	130.81 (19)	130.9	130.98
C4—C5—C10	122.7 (3)	123.63	123.55
O2—C1—O1	124.0 (2)	123.13	124.86
N1—N2—C11	116.81 (19)	116.41	116.36
C4—C5—C6	118.5 (2)	117.68	117.63
Dihedral angles (°)			
C3—C2—C1—O1	178.0 (3)	179.83	-178.93
C3—C2—C1—O2	-2.6 (5)	0.013	0.89
N1—C2—C1—O2	174.7 (3)	179.84	-178.85
N1—C2—C1—O1	-4.8 (5)	-0.335	1.32

Table 3

Experimental hydrogen-bond geometry values (Å, °)

D—H…A	D–H (Å)	H···A (Å)	D···A (Å)	D–H···A °
O1A—H1A…O2	0.87(4)	1.78(4)	2.656 (3)	179(4)
O1—H1…O2A	0.91(5)	1.76(5)	2.661 (3)	173(4)

Table 4

Hydrogen-bond geometry values on B3LYP/6-31G(d,p) (Å, °)

D—H…A	D–H (Å)	H···A (Å)	D···A (Å)	D–H···A °
O1A—H1A…O2	1.007	1.627	2.635	179.11
O1—H1…O2A	1.007	1.627	2.634	179.12

Table 5

Some experimental and calculated vibrational frequencies (cm^{-1}) and assignments of the compounds on B3LYP/6-31G(d,p).

	Experimental (cm^{-1})	B3LYP/6-31G(d,p)	
Assignments		Monomer (cm^{-1})	Dimer (cm^{-1})
ν OH	2990	3619	2995
ν CH	2955 - 3086	3081 - 3171	3080 - 3172
ν CH3	2594 - 2880	2947 - 3053	2947 - 3052
ν CO	1697	1753	1694
ν CC Benzene ring	1598	1588	1593
ν CN+ν CC Pyridazine ring	1544	1543	1546
ν CN+ν CC Pyrazole ring	1469	1430	1432
ν C-N-C + ν C-N-N pyrazole ring	1409	1399	1411
$\nu(O-CH_3)$	1009	1004	1003

Table 6

Experimental and theoretical ^{1}H and ^{13}C isotropic chemical shifts (with respect to TMS, all values in ppm) for the title compound

Atom	B3LYP/6-31G(d,p) (ppm)	Experimental (ppm)
H2	4.16	4.04
H5	3.89	4.04
H6	4.25	4.04
H4	6.83	7.52
H1	7.85	8.35
H7	5.77	13.23
H3	7.16	7.16
H28	7.24	7.34
H30	7.24	7.45
H32	8.81	7.34
H34	7.4	7.45
C26	53.98	55.74
C19	112.42	111.31
C17	121.54	120.92
C21	112.29	128.44
C16	124.47	128.94
C33	122.46	129.25
C29	122.31	129.25
C27	127.17	131.03
C31	131.56	131.03
C25	140.16	134.19
C23	144.42	144.65
C20	140.01	146.30
C18	150.17	152.79
C15	158.53	163.33
C24	154.73	165.36

Table 7

The calculated HOMO, LUMO energy values, HOMO – LUMO energy gap, electrophilicity index, electronegativity, chemical hardness and softness of the title compound

Parameters	Monomer form	Dimer form
HOMO (eV)	-6.45	-6.34
LUMO (eV)	-1.77	-1.75
$\lvert\Delta E\rvert$ (energy gap (eV)	4.68	4.59
χ (eV)	4.11	4.04
η (eV)	2.34	2.30
ζ (eV)	0.21	0.22
ψ (eV)	3.61	3.55

Table 8

Thermodynamic properties at different temperatures at B3LYP/6–31G(d,p) level

T (Kelvin)	H_m^o (kcal/mol)	$C_{p,m}^o$ (cal mol^{-1}K^{-1})	S_m^o (cal mol^{-1}K^{-1})
200	6.63	53.56	126.17
250	9.69	64.78	139.77
298.15	12.79	73.01	149.85
300	13.30	75.85	152.92
350	17.45	86.40	165.72
400	22.12	96.15	178.17
450	27.24	104.99	190.25
500	32.79	112.88	201.94

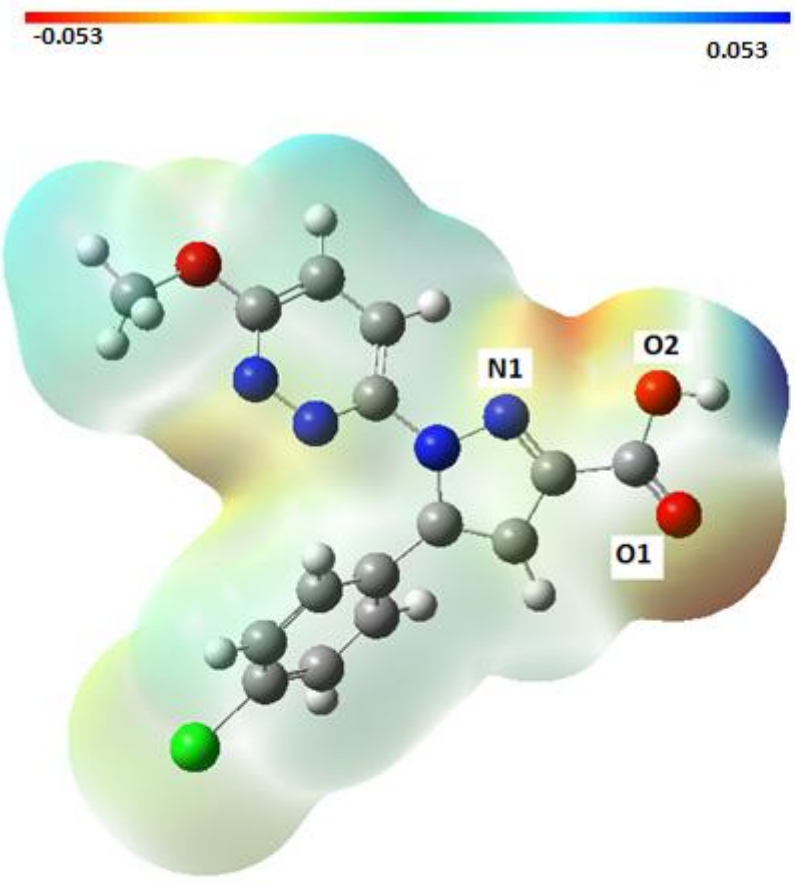

Monomer form

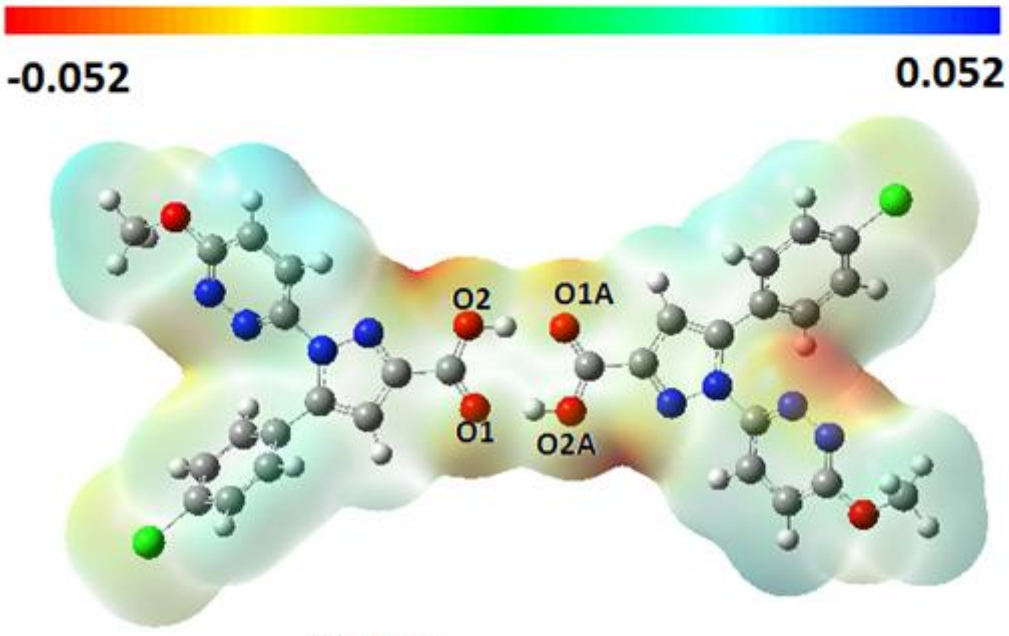

Dimer form

Highlights

- The title compound are re-synthesized and characterized experimentally and theoretically.
- Both monomer and dimeric form of The title compound are optimized by using B3LYP/6-31G(d,p)
- Observed and calculated values were compared.
- HOMO – LUMO, MEP map and Thermodynamic properties of the title compound are predicted.